Nuclear Instruments and Methods in Physics Research B 123 (1997) 193–198

NIM B
Beam Interactions with Materials & Atoms

ELSEVIER

First performance tests of VERA

A. Priller *, R. Golser, P. Hille, W. Kutschera, W. Rom, P. Steier, A. Wallner, E. Wild

Institut für Radiumforschung und Kernphysik, University of Vienna, Währinger Straße 17, A-1090 Wien, Austria

Abstract

VERA is a new 3-MV Pelletron tandem AMS facility in Vienna, which was installed during the last months of 1995. This report will discuss the performance characteristics of the facility established during the test operating phase and present first measurements of ^{14}C standards.

1. Introduction

VERA (Vienna Environmental Research Accelerator) is a new 3-MV Pelletron tandem AMS facility in Vienna (see corresponding contribution of Kutschera et al. [1]), which is currently in the test operation phase. The goal of this phase is to establish the conditions for performing AMS measurements of ^{10}Be, ^{14}C and ^{26}Al, and possibly ^{129}I. The basic components are designed to allow the extension of measurements to essentially all long-lived radionuclides up to the heaviest elements. The present paper describes its performance characteristics for measurements of light radionuclides. In this contribution we discuss the results obtained from ^{14}C measurements of some IAEA reference materials [2].

2. System configuration and performance

The VERA facility consists of a 3-MV Pelletron tandem accelerator manufactured by National Electrostatics Corporation (Middleton, Wisconsin, USA). A detailed layout of the AMS system is shown in Fig. 2 of Ref. [1]. At the low energy branch (injection site) there is an ion source of the cesium sputtering type for solid elements [3] holding 40 samples and sitting on a pre-acceleration potential of about 70 kV, a negative ion beam line with an electrostatic deflector (45°, $E/q = 92$ keV), a double-focusing injection magnet (90°, $ME/q^2 = 15$ MeV amu) for negative ions with insulated magnet chamber, necessary for sequential injection, and a multi Faraday-cup system with two offset cups for isotopes (molecules) lighter than the injected ion and one offset cup for a heavier isotope. VERA is designed for fast sequential injection by bouncing the electrically insulated magnet chamber. For typical ^{14}C measurements the system is set to inject ^{12}C for 0.5 ms followed by ^{13}C for 1.5 ms and ^{14}C lasting 98 ms. Including waiting periods the total cycle time is 120 ms. The magnet chamber of the low energy magnet is biased by about +300 V for all carbon isotopes in order to remove charges produced by interaction of the beam and the residual gas inside the chamber. Typical voltages applied to the magnet chamber are 11.6 kV (^{12}C) and 5.2 kV (^{13}C). In addition, there is a pair of X/Y-steerers circa half a meter before the accelerator entrance which can be biased by the sequencer depending on the isotope injected. For fast bouncing we use TREC P0705 and TREC 50/750 power supplies.

At the high energy beam line there is a double focusing magnet (90°, $ME/q^2 = 176$ MeV amu) for positively charged ions, an offset Faraday-cup system also with two cups for lighter isotopes and one for a heavier isotope, a foil stripper enabling one to strip the high energy ions again, and a switching magnet (at 20°, $ME/q^2 = 176$ MeV amu). In the direction straight through the switcher the beam line has a magnetic quadrupole doublet and a Wien filter $\boldsymbol{E} \times \boldsymbol{B} = 35$ kV/cm × 0.4 T). The particles are finally detected using a combination of a surface barrier detector and a Mylar foil (490 $\mu g/cm^2$ for separating ^{14}N from ^{14}C). The Wien filter effectively eliminates background ions still present in the beam after the analyzing magnet (Fig. 1a). ^{14}C can be clearly distinguished from ^{13}C and ^{14}N (Fig. 1b and Fig. 1c). The ^{14}N ions were produced by selecting mass-15 negative ions including $^{14}NH^-$ with the low-energy injection magnet, while the rest of the system was tuned for ^{14}C detection.

The Pelletron tandem accelerator is equipped with some features in order to reduce radiation due to the accelerator's operation. Around the accelerator tubes there are permanent magnets supplying a helical field of about 40 Gauss in the ion beam's path in order to suppress hard X-ray-radiation due to high-energy electrons produced in the strong electric field within the tubes. In addition, the vessel

* Corresponding author. e-mail priller@pap.univie.ac.at, fax +43 1 407 6200.

PII S0168-583X(96)00780-X

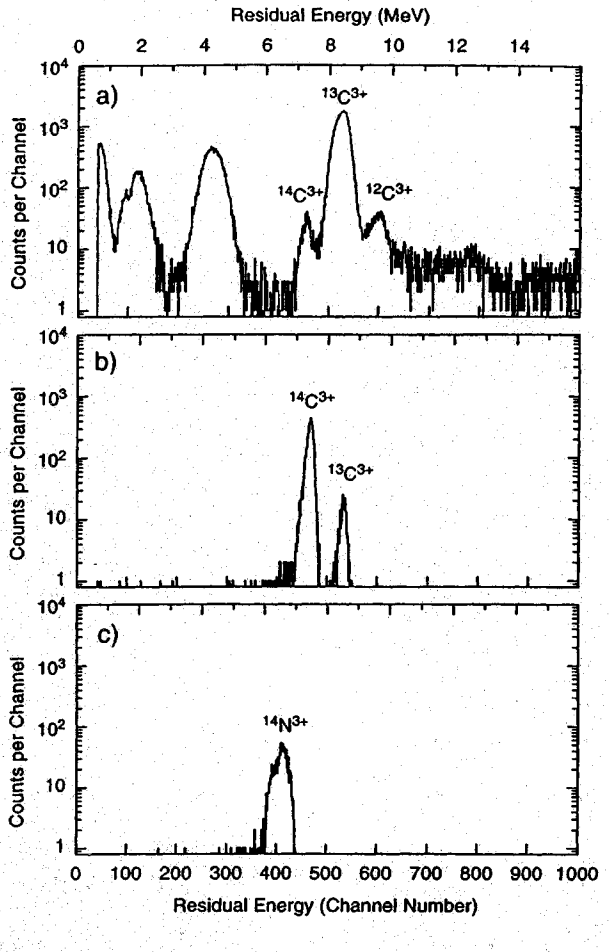

Fig. 1. Performance of the Wien filter. All particles entering the detector with the Wien filter off are shown by spectrum (a). The Wien filter on, spectrum (b) is obtained. The ^{14}N peak in spectrum (c) was generated by injecting $^{14}NH^-$ (see text).

containing the accelerating structure is wrapped with a 3.1 mm-thick lead sheet to reduce soft X-ray radiation (near the terminal the shield has its maximum thickness of about 2.9 cm). During normal ^{14}C operation, these two measures result in reducing the radiation to levels not significantly above background.

The terminal voltage is stabilized using both, the readout of the generating voltmeter and the sum of the output signals of two capacitive pick-offs on opposite sides of the terminal. Fig. 2 gives an idea of the time structure of the terminal voltage measured from the capacitive pick-off signal with a storage oscilloscope. It also shows the voltage drop of the terminal voltage when ^{12}C pulses are injected into the tandem. The $^{12}C^-$-peak current was 15 μA for this measurement. As can be seen from the figure this voltage drop is small compared to the overall terminal voltage variation. The slow variation of the terminal voltage is probably connected to the revolution time of the two charging chains (~ 0.3 s per revolution). The fast ripple seems to reflect the charging process of the terminal through the individual pellets (pellets arriving every 2.4 ms for each chain). The terminal voltage can also be stabilized using currents on the slits located after the high energy analyzing magnet in front of one of the offset cups. This stabilization system has not yet been used since the direct voltage stabilization system gave adequate voltage stability. The terminal of the accelerator is equipped with both a gas stripper and a foil stripper, which can be used separately or in combination. The reservoir of the stripper gas in the accelerator terminal can be refilled via a tubing leading from ground potential to the terminal site. The stripper gas assembly is split into two sections with the gas inlet and the foil stripper in the middle. The stripper canal

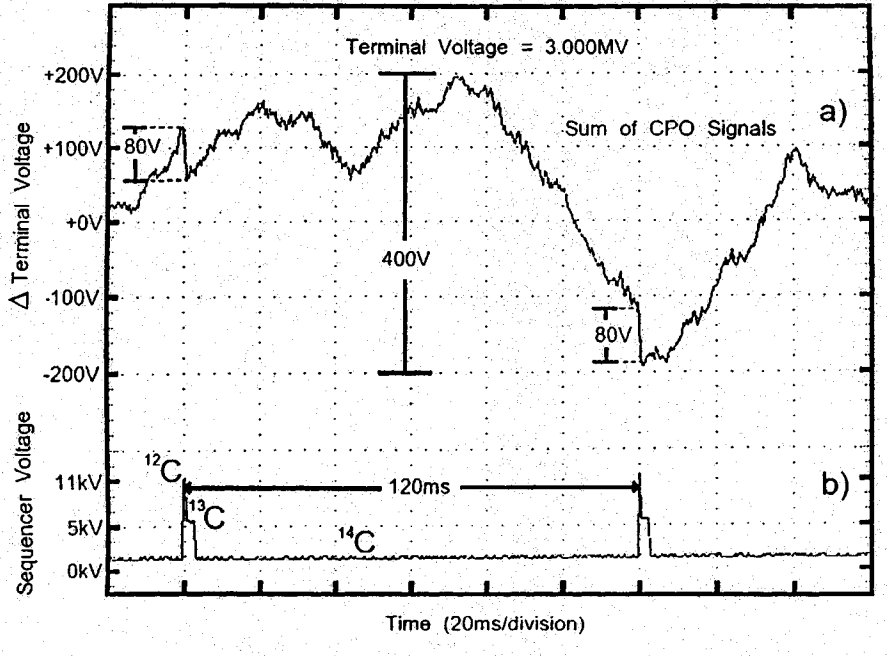

Fig. 2. Time structure of the tandem terminal voltage (a). The corresponding sequencer pulses are shown by curve (b).

Table 1
Ion beam currents measured behind the low energy analyzing magnet and the high energy analyzing magnet, respectively. The ions are produced using a 40-sample Cs-beam sputter source built by NEC, USA

Ion of interest	Injected ion	Low energy [μA]	Analyzed ion	High energy [particle μA]	$U_{terminal}$ [MeV]
^{11}B	$^{11}B_2^-$	2.9	$^{11}B^{2+}$	2.0	3.0
^{12}C	$^{12}C^-$	25.0	$^{12}C^{3+}$	10.0	3.0
^{27}Al	$^{27}Al^{16}O^-$	3.0	$^{27}Al^{2+}$	1.0	3.0
	$^{27}Al_2^-$	4.1	$^{27}Al^{2+}$	2.6	3.0
^{9}Be	$^{9}Be^{16}O^-$	2.5	$^{9}Be^{2+}$	0.87	3.0
^{197}Au	$^{197}Au^-$	14.8	$^{197}Au^{5+}$	0.24	3.0

on the low energy side has a diameter of 8 mm and is 384 mm long, whereas on the high energy side it has the same overall length and diameter but for the last 183 mm before the stripper exit its diameter is 9 mm (allowing for an increase in beam diameter due to multiple scattering in the stripper gas). At both ends of the stripper there is a turbo pump to recycle the stripper gas. At the entrance and the exit of the accelerator the pressure is about 4×10^{-8} Torr with the gas stripper (argon) adjusted for maximizing $^{12}C^{3+}$ ions at 2.7 MV terminal voltage.

Beam profile monitors are placed at several positions along the beam line in order to facilitate the tuning of VERA. They are located between the electrostatic deflector and the low-energy injection magnet near the entrance waist of the injection magnet, one after the accelerator near the entrance waist of the high energy analyzing magnet as well as one near the exit waist of this magnet and one between the Wien filter and the particle detector. The base pressure in the beam line system of VERA is kept in the low 10^{-9} Torr range with an all-cryopump system (seven pumps). All the facility is controlled by the VERA main computer (486 PC, 66 MHz), which allows one to operate VERA manually as well as automatically.

On 14 March 1996 the acceptance tests for specified beam currents were passed. Typical ion currents delivered by the source and measured behind the low-energy analyzing magnet as well as the ion currents behind the high-energy analyzing magnet are given in Table 1.

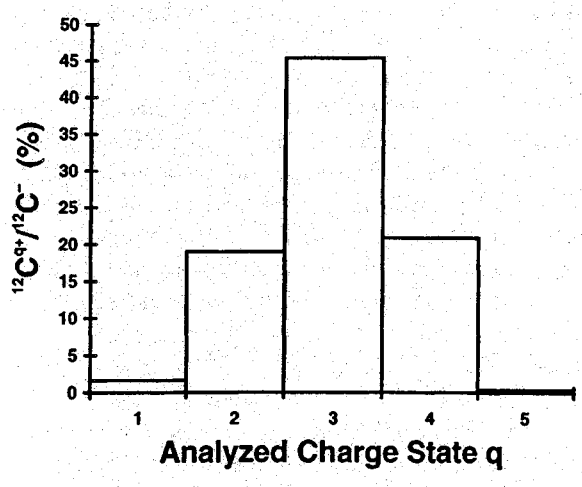

Fig. 3. Charge distribution for carbon measured with the high energy analyzing magnet. The stripper gas was argon and the terminal voltage was set to 2.7 MV.

The charge state distribution of ^{12}C ions was measured at 2.7 MV using argon as stripper gas at 4.9×10^{-3} Torr (measured at the center of the stripper canal). Fig. 3 displays the charge state distribution as measured in the straight cup after the analyzing magnet. Summing of the charge states from 1 + through 6 + leads to a total particle transmission of 87%.

3. ^{14}C measurements

A typical sequence for ^{14}C measurements proceeds as follows: ^{14}C is put into the accelerator, the ^{14}C detector is gated for taking data and the negative ion currents of masses 12 and 13 are measured in the two low-energy offset cups. When ^{12}C or ^{13}C is injected into the accelerator, its corresponding 3 + ion current is measured in the assigned high-energy offset cup. The actual cup currents are sampled shortly before the end of the current measuring period triggered by the sequencer controller and amplified by SRS SR570 current amplifiers.

The data are collected and stored in list mode as ASCII files by a separate computer (486 PC, 66 MHz) controlled by the main computer. For the present measurements, the final data visualization program was not yet available. Therefore data visualization was performed in parallel with a PC-based multichannel analyzer. The data are imported in a spread sheet program in order to display the currents and to build the ratios of $^{13}C^{3+}/^{12}C^-$, $^{13}C^{3+}/^{12}C^{3+}$ and $^{12}C^{3+}/^{12}C^-$. These ratios in combination with information gained from machine parameters logged for each run enables the quality control of the data. The spread sheet program is also used for calculating both, the $^{14}C^{3+}/^{12}C^{3+}$ and the $^{14}C^{3+}/^{13}C^{3+}$ ratios of the individual measurements.

In a first series of test runs, we measured oxalic acid II (HOxII) and some IAEA reference materials [2] such as C-3 cellulose, C-5 wood, and C-6 sucrose as well as "dead" carbon ($^{14}C/^{12}C \cong 6 \times 10^{-16}$ measured using VERA) put directly into one of the sample holders. The

same dead carbon was also used for producing a chemistry blank. All the samples were prepared in the new graphitisation system of VERA according to the method described by Vogel et al. [4]. For a typical sample preparation, a standard material with a carbon content of 5 mg was sealed in a quartz tube together with CuO (1 g) and some silver wire (~ 5 mg). Complete combustion to CO_2 was performed at a temperature of 900°C for two hours. The resulting CO_2 was cryogenically transferred to two separate reactor vessels. The reduction of CO_2 to elementary carbon was then performed with H_2 at 580°C using Co as catalyst (mass ratio Co/C ~ 3). Typical reduction times were 6 to 7 hours. Up to five individual ion source samples could be prepared from one reduction process. The sample holders for ^{14}C measurements were made out of aluminum, and the sample material was pressed into holes of 1 mm diameter, with a recession of 0.5 mm.

All the samples were loaded on one cathode wheel (made of copper), and were first conditioned by exposing them to the cesium beam for a few minutes. The samples were then measured seven times, each measuring period lasting 120 s including 1000 individual isotope cycles. The overall measuring time per sample was therefore 840 seconds. Typical ^{12}C-currents ranged between 15 and 30 μA producing a ^{14}C counting rate of up to 90 counts per second for the C-6 sucrose standard. Total ^{14}C counts collected per sample were in the range of 50 000. All ^{14}C measurements were performed at a terminal voltage of 2.7 MV. First, the $^{14}C^{3+}/^{12}C^{3+}$ ratios for the individual measurements were derived. The raw data was used for calculating the fraction modern of the standards and the chemistry blank as well as ratios between these standards.

In order to study the reproducibility and the influence of the sample position, a specific sample was split into several individual samples and put into different positions of the cathode wheel. The data of the seven runs of each individual sample were used to calculate the mean value (Eq. (1)) and its standard deviation (Eq. (2)).

$$\bar{x} = \frac{1}{n}\sum_{i=1}^{n} x_i, \tag{1}$$

$$\sigma = \sqrt{\frac{\sum_{i=1}^{n}(x_i - \bar{x})^2}{n(n-1)}}, \tag{2}$$

with $n = 7$ for our test runs.

From the standard deviation of the individual sample measurement its weight was calculated.

$$p = \left(\frac{1}{\sigma}\right)^2. \tag{3}$$

Then the weighted mean of the individual sample for a specific material (Eq. (4)), its external standard deviation (Eq. (5)) and its internal standard deviation (Eq. (6) were calculated (see also Fig. 4).

$$\bar{y} = \frac{\sum_{k=1}^{m} p_k \bar{x}_k}{\sum_{k=1}^{m} p_k}, \tag{4}$$

$$\sigma_{\text{ext}} = \sqrt{\frac{\sum_{k=1}^{m} p_k(\bar{x}_k - \bar{y})^2}{(m-1)\sum_{k=1}^{m} p_k}}, \tag{5}$$

$$\sigma_{\text{int}} = \sqrt{\frac{1}{\sum_{k=1}^{m} p_k}}, \tag{6}$$

with $m = 2$ to 5, the number of individual samples for a specific sample material (Fig. 4). The uncertainty given in Table 2 is the larger of the mentioned standard deviations.

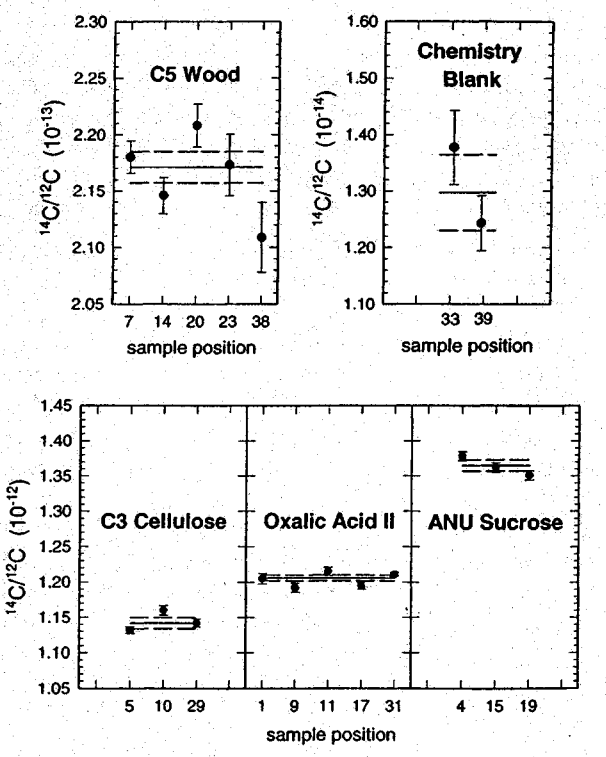

Fig. 4. First results of ^{14}C test runs with VERA. The measured $^{14}C/^{12}C$ ratios for individual samples are plotted at their respective sample position in the sample wheel. Each data point represents the mean value of seven runs (Eq. (1)) with its error bar and its standard deviation (Eq. (2)). The horizontal solid lines represent the weighted mean of the data points for each material (Eq. (4)). The dashed lines give the uncertainty of the weighted mean (Eq. (5) or Eq. (6), see text).

The uncertainty of the blank is dominated by counting statistics.

The results of the measurements were normalized to $\delta^{13}C = -25‰$ [5] and are given in Table 2.

$$\left(\frac{^{14}C}{^{12}C}\right)_{S,-25} = \left(\frac{^{14}C}{^{12}C}\right)_{S,x}\left(1 - \frac{2(25+x)}{1000}\right), \quad (7)$$

where $x = \delta^{13}C$ of the investigated sample material; S is the name of the sample material.

Finally, the fraction modern of the chemistry blank (Eq. (8)) and of the sample material (Eq. (9)) corrected for chemistry blank contribution were calculated [5].

$$\left(\frac{\left(\frac{^{14}C}{^{12}C}\right)_{B,-25}}{\left(\frac{^{14}C}{^{12}C}\right)_{ON}}\right) = \frac{\left\{\left(\frac{^{14}C}{^{12}C}\right)_{B,-25}\right\}_{meas}}{0.7459\left(\left(\frac{^{14}C}{^{12}C}\right)_{HOxII,-25} - \left\{\left(\frac{^{14}C}{^{12}C}\right)_{B,-25}\right\}_{meas}\right)}, \quad (8)$$

$$\left(\frac{\left(\frac{^{14}C}{^{12}C}\right)_{S,-25}}{\left(\frac{^{14}C}{^{12}C}\right)_{ON}}\right) = \frac{\left(\left\{\left(\frac{^{14}C}{^{12}C}\right)_{S,-25}\right\}_{meas} - \left\{\left(\frac{^{14}C}{^{12}C}\right)_{B,-25}\right\}_{meas}\right)}{0.7459\left(\left(\frac{^{14}C}{^{12}C}\right)_{HOxII,-25} - \left\{\left(\frac{^{14}C}{^{12}C}\right)_{B,-25}\right\}_{meas}\right)}, \quad (9)$$

where B = chemistry blank, S = name of the sample, and

$$\left(\frac{^{14}C}{^{12}C}\right)_{ON} = 0.95\left(\frac{^{14}C}{^{12}C}\right)_{HOxI}\left(1 - \frac{2(19+\delta^{13}C)}{1000}\right). \quad (10)$$

The background correction only considers contamination by ^{14}C during chemical preparation.

4. Discussion of the results

The terminal voltage has been set to 2.7 MV for the measurements mentioned in the previous chapter. Table 2 shows a comparison between the measured $^{14}C/^{12}C$ ratios of several standards and the absolute values of these standards in 1996. The latter were calculated from the activity of the "old" oxalic acid (now called HOxI), which is given as 14.27 dpm/(g carbon) for 1950 AD [6]. This leads to a 1950 standard activity of $A_{ON} = 0.95 A_{HOxI} = 13.56$ dpm/(g carbon), which translates into $^{14}C/^{12}C = 1.189 \times 10^{-12}$. Correcting for decay from 1950 to 1996, one obtains $^{14}C/^{12}C = 1.181 \times 10^{-12}$. This value was used to calculate the absolute standard values in the last column of Table 2 using the known relation between HOxI and HOxII, and the fraction-of-modern-carbon values of Table 3 for the IAEA standards. For this comparison, the C-6 sucrose was normalized to $\delta^{13}C = -25‰$. The comparison of the absolute $^{14}C/^{12}C$ ratios in Table 2 gives a measure of the relative detection efficiency for the $^{14}C/^{12}C$ ratio measurements. As can be seen from Table 2, the measured ratios are considerably smaller. Since we observed a much smaller deviation for another series of test runs at a terminal voltage of 3.0 MV (not reported here), we currently ascribe these lower $^{14}C/^{12}C$ ratios at 2.7 MV to a shift in the 3+ charge state fractionation in the terminal stripper gas (the stable isotope ratio $^{13}C/^{12}C$ showed a similar trend). However, using the charge state distribution measured for argon stripper gas [7], we cannot account for the difference, since at TV = 2.7 MV an almost equal $^{14}C^{3+}$ and $^{12}C^{3+}$ charge state fraction is expected [7]. It seems unlikely that the relative detection efficiency between the ^{12}C current measurement and the ^{14}C detection has changed by much between a terminal voltage of 3.0 MV and 2.7 MV, although one can think of many factors which influence this efficiency ratio (e.g. change of emittance coupled with a change of transmission, etc.). As is well known, absolute $^{14}C/^{12}C$ ratio measurements are not required for ^{14}C measurements. However, it seems useful for both quality control [8] and a

Table 2
Results of the measurements of ^{14}C standards from IAEA (C-3, C-5, C-6 [2]), and of oxalic acid II (HOxII). The uncertainties in column 3 were calculated with Eqs. (5) and (6). For comparison the uncertainty due to counting statistics is given in column 4. The absolute $^{14}C/^{12}C$ ratios for 1996 AD were calculated from the standard values and the absolute activity of oxalic acid I (HOxI) given in Ref. [6]. Both measured and calculated ratios are normalized to $\delta^{13}C = -25‰$

Sample	$(^{14}C/^{12}C)_{measured}$ $[10^{-12}]$	Uncertainty [%]	Statistical uncertainty [%]	$(^{14}C/^{12}C)_{absolute}$ $[10^{-12}]$
C-6 sucrose	1.326	0.59	0.25	1.730
C-5 wood	0.2173	0.64	0.48	0.2727
C-3 cellulose	1.142	0.68	0.26	1.530
HOxII	1.189	0.34	0.20	1.608

Table 3
Comparison of measured and nominal ^{14}C fractions in units of percent modern carbon (pMC). The measured fractions are calculated with Eqs. (8) and (9)

Sample	Measured fraction [pMC]	Uncertainty [%]	Nominal fraction [pMC]	Relative difference [%]
Chemistry blank	1.48	5.25		
C-6 sucrose	149.7	0.69	150.6	−0.59
C-5 wood	23.31	0.81	23.05	1.11
C-3 cellulose	128.7	0.77	129.4	−0.55

deeper understanding of a new AMS system. Clearly, more measurements are needed to clarify the situation.

In Table 3, $^{14}C/^{12}C$ ratios normalized in the usual way [5] are compared with nominal values. As can be seen the measured and the nominal values agree reasonably well. Only wood differs by more than 1% from its corresponding nominal value. However, this may be due to the relatively large background correction. It should be noted that, at this stage, both the chemistry blank and the other samples were prepared without pre-treatment of the CuO. This may explain the relatively high blank value. Measurements of "dead" carbon put directly into the ion source gave $^{14}C/^{12}C$ ratios an order of magnitude lower than the chemistry blank. From many measurements with "dead" graphite samples between runs with modern ones it was also observed that no cross contamination at a level $> 10^{-3}$ occurred.

5. Conclusion

The results reported in this paper have to be considered as preliminary, since they represent measurements only half a year after installation of the entirely new AMS systems. In view of this, the achieved precision for $^{14}C/^{12}C$ ratio measurements is encouraging and tells us that the whole system is already working close to expectation. As time goes on, we expect a gradual improvement of the system which should be capable of both high-precision ^{14}C measurements ($\sim 0.5\%$) and measurements with other radionuclides.

Acknowledgements

The continued help of Max Cichon and Robert Daniel from NEC during installation and test runs of VERA is gratefully acknowledged.

References

[1] W. Kutschera, P. Collon, H. Friedmann, R. Golser, P. Hille, A. Priller, W. Rom, P. Steier, S. Tagesen, A. Wallner, E. Wild and G. Winkler, these Proceedings (AMS7), Nucl. Instr. and Meth. B 123 (1997) 47.
[2] Rozanski, IAEA Quality Assurance Materials (IAEA, Vienna, 1991).
[3] J.A. Ferry, Nucl. Instr. and Meth. A 328 (1993) 28.
[4] J.S. Vogel, J.R. Southon, D.E. Nelson and T.A. Brown, Nucl. Instr. and Meth. B 5 (1984) 289.
[5] M. Stuiver and A. Polach, Radiocarbon 19/3 (1977) 355.
[6] I. Karlén, I.U. Olsson, P. Kållberg and S. Kilicci, Arkiv för Geofysik 4/22 (1964) 465.
[7] G. Bonani, P. Eberhardt, Th.R. Niklaus, M. Suter, H.A. Synal and W. Wölfli, Nucl. Instr. and Meth. B 52 (1990) 338.
[8] R.J. Schneider, A.P. McNichol, M.J. Nadeau and K.F. von Reden, Radiocarbon 37/2 (1995) 693.